BIOCHEMISTRY
including biophysical chemistry & molecular biology

Article

pubs.acs.org/biochemistry

# Effect of Salt Concentration on the Conformation of TAR RNA and Its Association with Aminoglycoside Antibiotics

Amy L. Smith,[†] Joseph Kassman,[‡,§] Khalid J. Srour,[†] and Ana Maria Soto*[,†]

[†]Department of Chemistry, Towson University, Towson, Maryland 21252, United States

[‡]Department of Chemistry, The College of New Jersey, Ewing, New Jersey 08628, United States

**ABSTRACT:** RNA is an important biological target because it plays essential roles in many pathogenic and normal cellular processes. The design of inhibitors that target RNA involves optimization of noncovalent interactions, including van der Waals, hydrogen bond, and electrostatic interactions. Although sometimes regarded as nonspecific, electrostatic interactions are important in this optimization because the specific position of the phosphates may allow for specific charge−charge interactions with bound ligands. In this work, we have investigated the contribution of electrostatic interactions to the binding affinity of aminoglycoside antibiotics for TAR RNA. Because the charges in aminoglycoside antibiotics are provided by protonated amino groups, it is difficult to separate the contribution of hydrogen bonds and electrostatics to their binding specificity. Hence, we have investigated the dependence of the binding affinity on salt concentration, which should affect only the electrostatic contributions. Our results show that four aminoglycoside antibiotics (paromomycin, kanamycin-B, gentamycin, and tobramycin) bind TAR RNA with different affinities. Furthermore, the dependence of the binding affinity on salt concentration is different for kanamycin-B and paromomycin, with kanamycin-B showing a stronger dependence. Because all these antibiotics contain five positive charges, the results suggest that each antibiotic orients its charges in different ways when bound to TAR RNA. Our overall results support the idea that charge−charge interactions can contribute significantly to the specific binding of antibiotics to TAR RNA. Hence, the exact position of the charges should be considered in the design of any inhibitor of the interactions of TAR RNA.

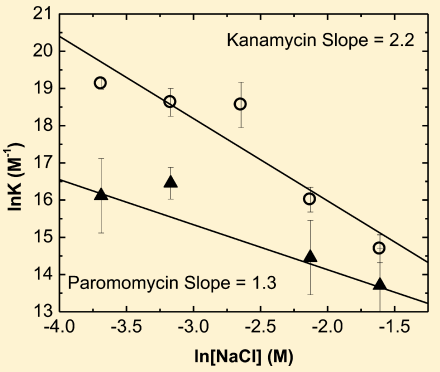


In recent years, it has been discovered that RNA plays important roles in many cellular processes, including transcription, translation, and splicing.[1] Furthermore, many RNAs are related to diseases, either due to mutations that affect their normal function[1] or because they are part of pathogenic organisms that invade our cells.[2] Hence, RNA is an important target for the design of inhibitors directed at preventing pathological processes.[3] One such target is TAR RNA, a 59-nucleotide fragment from the human immunodeficiency virus-1 (HIV-1) genome that forms a stem loop containing an internal bulge.[4−6]

The pathogenesis of HIV-1 follows many steps requiring the use of viral as well as host enzymes.[2,7,8] After the virus has fused with the membrane, the viral RNA genome is released into the host cells, where the viral enzymes "reverse transcriptase" and "integrase" facilitate its conversion to a DNA duplex and its integration into the host genome.[2,7] Subsequently, the host's RNA polymerase is recruited to transcribe the viral genes. This process is initially of very low efficiency;[2,9] however, after synthesis of the first few RNA nucleotides, a region called the transactivator responsive region (TAR) folds into a hairpin structure, which is recognized by the viral protein Tat.[10−12] Binding of Tat to TAR also brings other factors into the complex, including p-TEFb (composed of cyclin T1 and the CDK9 kinase),[13] which ultimately phosphorylates the C-terminus of eukaryotic RNA polymerase,[14] dramatically increasing the number of full-length transcripts.[15] In the absence of Tat, RNA polymerase stalls, yielding only incomplete transcripts. Thus, there is significant interest in finding drugs that could prevent the interactions between TAR and Tat.

The design of inhibitors that target RNA involves optimization of noncovalent interactions, including van der Waals, hydrogen bond, and electrostatic interactions.[16] Electrostatic interactions are important for increasing the binding affinity through long-range charge−charge interactions and through the increase in entropy resulting from the release of counterions.[17] However, the position of the phosphates resulting from the specific RNA conformation allows for electrostatic complementarity, resulting in specific charge−charge interactions.[16,17] Aminoglycoside antibiotics bind TAR[18] and result in a conformational change that is incompatible with Tat binding,[19,20] thereby preventing the proliferation of HIV-1. It has been proposed that aminoglycoside antibiotics are able to selectively bind RNA targets by exploiting this electrostatic complementarity.[16] However, because the charges in aminoglycoside antibiotics are given by protonated amino groups,[21] which can make hydrogen bonds with RNA groups, it is difficult to separate the contribution of hydrogen bonds and

**Received:** May 31, 2011
**Revised:** August 21, 2011
**Published:** September 14, 2011

  

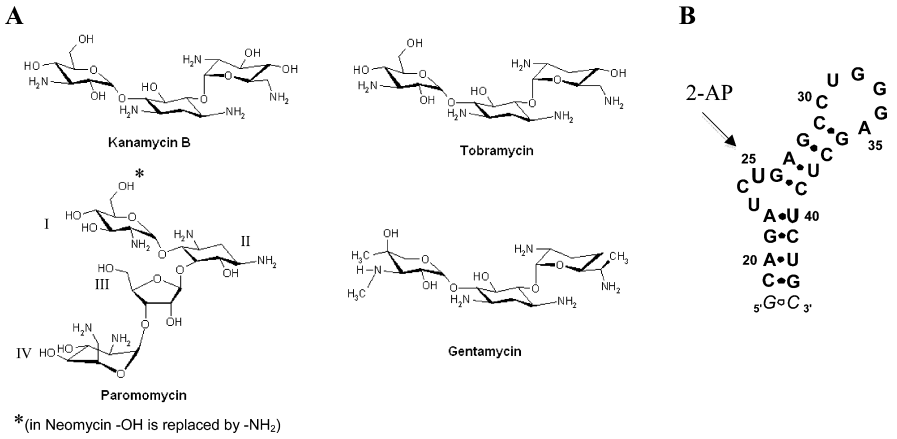


**Figure 1.** Structures of the molecules used in this work: (A) aminoglycoside antibiotics and (B) TAR RNA. U25 was replaced with 2-aminopurine in fluorescence experiments. The last GC base pair (G18-C44) is inverted with respect to the original TAR sequence.

electrostatics to their binding specificity. In this work, we have investigated the contribution of electrostatic interactions to the binding affinity of selected aminoglycoside antibiotics by investigating the dependence of the binding affinity on salt concentration, which should affect only the electrostatic contributions.

We have initially compared the binding of four aminoglycosides to TAR RNA: paromomycin, gentamicin, tobramycin, and kanamycin-B. All aminoglycosides contain five charges, but they are positioned in different parts of the molecules (Figure 1). After initial characterization, we focused on kanamycin-B and paromomycin for determining the dependence of the binding affinity on salt concentration. Because the conformation of the RNA places its electronegative groups at specific positions in space, its asymmetric electrostatic field may be recognized by specific ligands.[22,23] Hence, the spatial distribution of the aminoglycoside charges may affect their binding affinity ($K$) if these charges are indeed contributing to their binding specificity. Aminoglycosides with charges in an optimal position to interact with the charges of TAR will exhibit the highest affinity at low ionic strengths and, most importantly, the greatest dependence of $K$ on salt concentration. Our results show that kanamycin-B binds TAR with greater affinity than paromomycin. Furthermore, the salt dependence of kanamycin-B is stronger than that of paromomycin, suggesting that the amino groups in kanamycin-B are better positioned for specific charge−charge interactions with TAR. Our results have implications for the design of inhibitors of the interactions between TAR and Tat. Although aminoglycosides bind TAR with only modest affinities (micromolar to millimolar range), understanding the principles of their recognition can lead to the development of molecules that bind TAR with higher affinities.

## EXPERIMENTAL PROCEDURES

**Materials.** All antibiotics were purchased from Sigma-Aldrich and used without further purification. Unmodified TAR RNA was purchased from Integrated DNA Technologies (Coralville, IA) and was purified by a combination of gel electrophoresis and electroelution. TAR modified with a 2-aminopurine base was synthesized and purified by Dharmacon, Inc. (Chicago, IL).

**UV Melts.** Absorbance versus temperature profiles were collected in a thermoelectrically controlled Cary 100 UV−vis spectrophotometer, equipped with a Peltier temperature controller, using wavelengths of 260 and 280 nm and a temperature range of 15−98 °C. Unfolding enthalpies ($\Delta H_{unfold}$) were obtained assuming that TAR RNA unfolds in two consecutive two-state transitions. An initial estimate of $\Delta H_{unfold}$ was obtained by applying the following equations to the first derivatives of the unfolding profiles, as described previously:[24] $\Delta H = B/(1/T_1 - 1/T_2)$ or $\Delta H = B'/(1/T_M - 1/T_2)$, where $B$ and $B'$ are constants corresponding to the molecularity of the transition (for monomolecular transitions, $B = -7$ and $B' = -3.5$), $T_M$ is the temperature (in kelvin) at which the change in absorbance ($\partial A/\partial T$) is maximal, and $T_1$ and $T_2$ are the lower and upper temperatures, respectively (in kelvin), at which the change in absorbance is equal to half of the maximum. More accurate unfolding enthalpies and $T_M$ values for each transition were obtained using Global Melt Fit, developed by D. Draper.[25,26]

**Differential Scanning Calorimetry.** The model-independent unfolding enthalpy of TAR at low $Na^+$ concentrations was obtained using a VP-DSC instrument from Microcal, Inc. In a typical experiment, a 0.04 mM solution of TAR RNA was placed in the sample compartment and a buffer solution with the exact same $Na^+$ and $H^+$ concentrations was placed in the reference compartment. The RNA was unfolded by increasing the temperature at a rate of 30 °C/h. Five consecutive scans were conducted with pre-equilibration times of 30 min between scans; an experiment was deemed successful when the last four curves were superimposable. A baseline (created by filling the sample and reference compartments with the buffer solution) was subtracted from the sample unfolding profile. The resulting curves were normalized for concentration and integrated to obtain model-independent enthalpies of unfolding.

**Circular Dichroism (CD) Titrations.** CD experiments were conducted in a Jasco J810 spectropolarimeter equipped with a Peltier temperature controller. We followed the conformation of TAR upon addition of $Mg^{2+}$ by monitoring the CD signal at 222 nm and correcting the signal for dilution. The binding affinity of the various antibiotics for TAR RNA at 140 mM $Na^+$ was obtained as follows: 2000 μL of a solution containing ~4 μM TAR, 10 mM MOPS (pH 7), and 140 mM NaCl was placed on a standard quartz cuvette; 1−60 μL aliquots of a solution containing the corresponding antibiotic (~0.2 mM), 10 mM MOPS (pH 7), and 140 mM NaCl were added to the cuvette, and the CD signal at 222 nm was measured. The signal was corrected for dilution, and the binding affinities were obtained by fitting the resulting binding

isotherms (CD vs concentration profiles) to the following equation:

$$A = \left(\left\{[\mathrm{Tar}] + [\mathrm{Abt}] + 1/K - \sqrt{([\mathrm{Tar}] + [\mathrm{Abt}] + 1/K)^2 - 4[\mathrm{Tar}][\mathrm{Abt}]}\right\}/(2[\mathrm{Tar}])\right)(A_b - A_f) + A_f \quad (1)$$

where [Tar] and [Abt] represent the total TAR and antibiotic concentrations, respectively, $A$ represents the CD signal at 222 nm, and $A_f$ and $A_b$ are the signals at the beginning and end of the experiment, respectively. Each titration was conducted at least two times, and the binding isotherms were fitted using Origin (OriginLab, Northampton, MA).

**Fluorescence Titrations.** Binding affinities in the presence of 0.1 mM $MgCl_2$ were measured using a modified RNA containing 2-aminopurine (2-AP) in position 25, as described by Bradrick and Marino[27] but with some modifications to account for the slight change in conformation resulting from the incorporation of 2-AP, as described previously for other RNAs.[28] Briefly, two solutions were prepared: one containing AP-TAR alone and one containing a combination of AP-TAR and unmodified TAR. For the AP-TAR and unmodified TAR combination, 1500 $\mu$L of a solution containing 0.162 $\mu$M AP-TAR RNA, 0.158 $\mu$M unmodified TAR RNA, 10 mM MOPS (pH 7), and NaCl concentrations ranging from 42 to 334 mM was heated to 90 °C for 7 min and immediately cooled on ice for 7 min. The solution was then transferred to a fluorescence cuvette; 0.00025 mmol of $MgCl_2$ was added, and the solutions were diluted to 2500 $\mu$L using 10 mM MOPS (pH 7) to yield final AP-TAR and unmodified TAR concentrations of 0.097 and 0.095 $\mu$M, respectively, 0.1 mM $MgCl_2$, and NaCl concentrations ranging from 25 to 200 mM. Solutions containing AP-TAR alone were prepared in the same way; however, 0.324 $\mu$M AP-TAR (instead of 0.162 $\mu$M) was used, and the unmodified TAR was not included. Aminoglycoside antibiotics were prepared and calibrated as described below. In a typical titration, a 10 $\mu$M solution of antibiotic was added using increments of 1−100 $\mu$L. Each addition was measured in a Jovin Yvon spectrofluorometer using excitation at 310 nm, and the emission was collected at three points: 375, 384, and 390 nm. Each titration was conducted at least twice. At $Na^+$ concentrations of >100 mM, the resulting binding isotherms (fluorescence vs concentration profiles) were fitted to a single-site binding isotherm using eq 1 (shown above). In eq 1, [Tar] and [Abt] represent the total concentrations of RNA and antibiotic at a given point, respectively, $K$ is the binding affinity, $A$ is the fluorescence intensity at a given point, $A_b$ is the final fluorescence (when all RNA is bound) and $A_f$ is the fluorescence at the beginning of the experiment [when all RNA is free (unbound)]. Binding isotherms were fitted using Origin or ProFit (Quantum Soft), allowing $K$, $A_b$, and $A_f$ to float until the best fit was found.

At the lower NaCl concentrations, a secondary binding site with a weak affinity was observed. In those cases, the first few data points were fitted to a single-site binding isotherm (eq 1) to obtain an approximate binding affinity. More accurate binding affinities were obtained using ProFit (Quantum Soft), by fitting the fluorescence binding isotherms to a two-site binding model, as previously described.[29−31] The two-site binding model can be briefly summarized as follows. It was assumed that each TAR molecule contained two independent binding sites for the antibiotics, one of high affinity ($K_1$) and one of low affinity ($K_2$). If we assume that $K_1 \gg K_2$, the fractions of free RNA and antibiotic bound to each site (labeled $\theta_{free}$, $\theta_1$, and $\theta_2$) can be calculated on the basis of the binding affinities, and the concentration of free antibiotic (labeled $[\mathrm{Abt}]_{free}$), according to the following equations:

$$\theta_{free} = 1 - \theta_1 \quad (2)$$

$$\theta_1 = \frac{K_1[\mathrm{Abt}]_{free}}{1 + K_1[\mathrm{Abt}]_{free}} \quad (3)$$

$$\theta_2 = \frac{K_2[\mathrm{Abt}]_{free}}{1 + K_2[\mathrm{Abt}]_{free}} \quad (4)$$

Once $\theta_{free}$, $\theta_1$, and $\theta_2$ are obtained, the fluorescence ($I_F$) can be calculated using different coefficients for each species as follows:

$$I_F = \theta_1\varepsilon_{TAR\_bound1} + \theta_2\varepsilon_{TAR\_bound2} + \theta_3\varepsilon_{TAR\_free} \quad (5)$$

where $\varepsilon_{TAR\_bound1}$, $\varepsilon_{TAR\_bound2}$, and $\varepsilon_{TAR\_free}$ are coefficients relating the fluorescence signal to the concentrations of TAR bound to the first ligand, TAR bound to the second ligand, and unbound TAR, respectively.

The procedure described above requires that the free antibiotic concentrations be known. The concentration of free antibiotic can be calculated from the total RNA concentration, $K_1$, $K_2$, and the total antibiotic concentration,[29,30] using the following equation, as previously described:[31]

$$[\mathrm{Abt}]_{free} = -\frac{U}{3} + \frac{2}{3}\left(\cos\frac{T}{3}\right)\sqrt{U^2 - 3S} \quad (6)$$

where $S = 1/K_1K_2 + [\mathrm{RNA}]_{total}(1/K_1 + 1/K_2) - [\mathrm{Abt}]_{total}(1/K_1 + 1/K_2)$, $U = 1/K_1 + 1/K_2 + 2[\mathrm{RNA}]_{total} - [\mathrm{Abt}]_{total}$, and $T = \arccos([-2U^3 + 9US - (27[\mathrm{Abt}]_{total}/K_1K_2)]/\{2[(U^2 - 3S)^3]^{1/2}\})$

Equations 2−6 were combined into one equation and used to fit the data using ProFit (Quantum Soft). To start the fitting, the value of $K_1$ was set to the value obtained from fitting the initial points of the binding curve and the value of $K_2$ was set to be approximately 50 times smaller. Initial guesses for the extinction coefficients were obtained from the fluorescence values of experimental data ($\varepsilon_{TAR\_bound1}$ approximates the lowest value; $\varepsilon_{TAR\_bound2}$ approximates the final value; $\varepsilon_{TAR\_free}$ approximates the initial value).

**Aminoglycoside Concentrations.** Once in solution, aminoglycosides degrade relatively quickly. Hence, aminoglycoside solutions were prepared daily, by dissolving appropriate weights in the same buffer as the RNA molecules [10 mM MOPS (pH 7), 0.1 mM $MgCl_2$, and NaCl concentrations ranging from 25 to 200 mM]. Initial concentrations were determined using the reported molecular weight of the antibiotics, but these were deemed approximate because the sulfate content of most antibiotics is not accurately known. Accurate concentrations were determined by conducting pH titrations, using standardized KOH solutions. The end point of the titration was used to determine the concentration of amino groups and to calculate an exact molecular weight of each antibiotic. These titrations were also useful to estimate the $pK_a$ values of each antibiotic. In a typical titration, 3.5−5 mL of a

25−50 mM solution of antibiotic in water was placed in a container. A measured amount of 12 M HCl was added until the pH was 1, and a 1 M KOH solution was added using increments of 2−100 μL. The pH was recorded after each addition until a pH of 12 was reached. Titrations were analyzed by examining $\partial$pH/$\partial$[KOH] versus [KOH] plots. Each plot exhibits two peaks: the first one corresponds to the complete neutralization of excess HCl and marks the beginning of the amino group titration; the second peak corresponds to the complete neutralization of amino groups. The concentration of KOH required to go from the first to the second peak was used to determine the concentration of free amino groups present in solution. After taking into account the number of amino groups per antibiotic and all the dilutions from adding the HCl and KOH, the concentration of free amino groups was used to back-calculate the initial concentration of antibiotic and to estimate an accurate molecular weight to be used in subsequent experiments.

**RNA Concentrations.** RNA stock concentrations (in water) were obtained by measuring the absorbance at 260 nm and 80 °C, using an extinction coefficient of 251.8 $cm^{-1}$ $mM^{-1}$ for both the wild type and 2-aminopurine-modified TAR. Concentrations were also measured at room temperature and 260 nm after digestion of the RNA in 0.2 M NaOH for 14 h, at 40 °C and using extinction coefficients corresponding to the mixture of nucleotides ($\varepsilon_{AP\text{-}TAR}$ = 277.4 $cm^{-1}$ $mM^{-1}$, and $\varepsilon_{TAR}$ = 286.3 $cm^{-1}$ $mM^{-1}$, calculated using the following values for the extinction coefficients of the free bases: 15.4 $cm^{-1}$ $mM^{-1}$ for A, 9.9 $cm^{-1}$ $mM^{-1}$ for U, 7.5 $cm^{-1}$ $mM^{-1}$ for C, and 11.7 $cm^{-1}$ $mM^{-1}$ for G;[32] 2-AP = 1[33]). Both methods give the same concentrations, within error.

## RESULTS

**RNA Molecules.** The fragment of TAR used in these studies (Figure 1B) consists of nucleotides 18−44 of the full-length TAR structure, which has been extensively analyzed.[27,34] The last GC base pair (G18-C44) of this TAR model was inverted with respect to the original TAR sequence to keep the molecule consistent with the studies of Marino[27] and Crothers[34] (this last base pair was inverted in previous studies to improve transcription efficiency). On the basis of the structure of the neomycin−TAR complex,[19] the TAR RNA fragment used in our studies should contain a full neomycin site. The structures of neomycin, paromomycin, tobramycin, kanamycin-B, and gentamycin are shown in Figure 1A. With the exception of neomycin, which has six charges, all the antibiotics used in this work contain five amino groups that should be charged to a similar extent at pH 7 (as discussed below).

**TAR RNA Folding.** Before comparing the binding of aminoglycoside antibiotics to TAR RNA, we needed to determine the conditions under which TAR RNA is fully folded. Although the structure of TAR RNA is simple, there are enough tertiary contacts[35] that the presence of different salt concentrations could result in the formation of different starting structures. In fact, the relative orientation of the helices and the stacking interactions at and around the three-nucleotide bulge can vary significantly under various ionic conditions.[36] Indeed, the binding affinity of neomycin (measured in circular dichroism titrations) as a function of $Na^+$ results in a bell-shaped plot (Figure 2), suggesting that in the absence of $Mg^{2+}$, TAR RNA does not fully fold at low $Na^+$ concentrations, preventing neomycin from fitting properly into its binding site and resulting in a low binding affinity. As the concentration of $Na^+$ increases, the RNA is better folded, allowing neomycin to fully interact with TAR RNA (observed as an increase in affinity). Once the RNA is completely folded (~140 mM $Na^+$), excess $Na^+$ interferes with the RNA−neomycin charge−charge interactions and the affinity decreases.

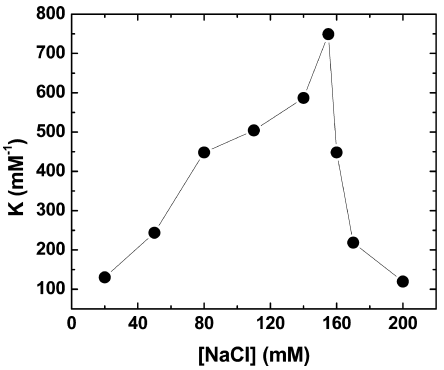


**Figure 2.** Binding of neomycin to TAR RNA at various NaCl concentrations. All experiments were conducted at 25 °C in 10 mM MOPS (pH 7) and NaCl concentrations ranging from 20 to 200 mM.

**Effect of $Mg^{2+}$ on the Conformation of TAR RNA.** Figure 3 shows the change in ellipticity at 222 nm of TAR RNA as the concentration of $Mg^{2+}$ increases. The results show that after ~0.08 mM $Mg^{2+}$, the conformation of TAR does not change with increasing $Mg^{2+}$ concentrations, suggesting that ~0.1 mM $Mg^{2+}$ is enough to completely fold TAR RNA.

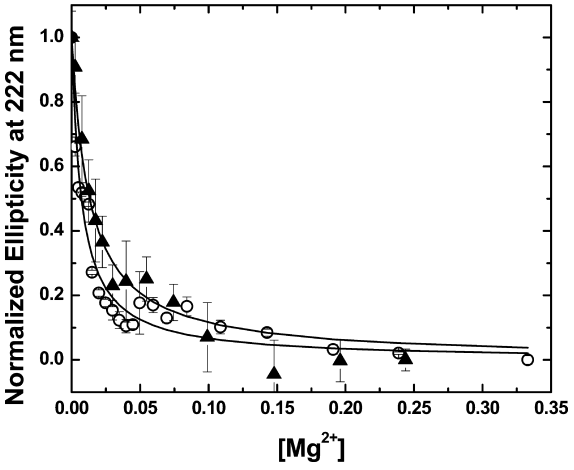


**Figure 3.** Conformational changes in TAR RNA upon addition of $MgCl_2$. Results from two replicate experiments are shown. TAR RNA was dissolved in 10 mM MOPS (pH 7) and titrated with 5−10 mM $MgCl_2$, also dissolved in 10 mM MOPS (pH 7), at room temperature.

**UV Melts.** UV melts at different $Na^+$ concentrations (Figure 4A and Table 1) show that the conformation of TAR changes as the concentration of $Na^+$ increases. At a low $Na^+$ concentration (25 mM), a single transition is observed, but as the concentration of $Na^+$ increases, the presence of two transitions becomes increasingly clear. Two transitions are expected if the two helical regions of TAR (Figure 1) unfold independently. The helices are expected to have slightly different stabilities because they have different sequences and lengths. Calorimetry experiments (see below) suggest that even the single transition observed at low $Na^+$ concentrations is


dx.doi.org/10.1021/bi200835t | Biochemistry 2011, 50, 9434−9445

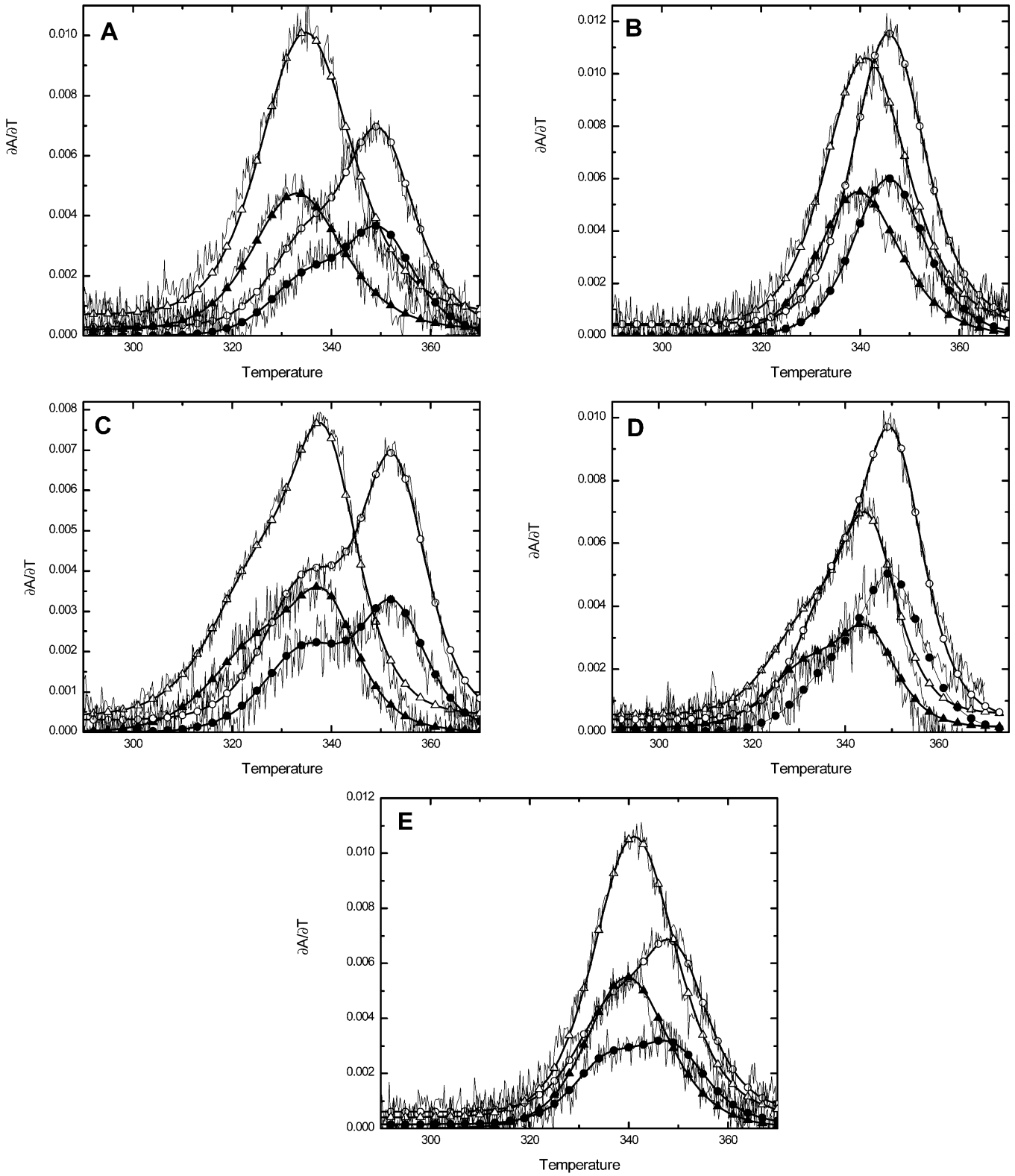


**Figure 4.** UV unfolding profiles of TAR and AP-TAR at 260 nm (filled symbols) and 280 nm (empty symbols). All experiments were conducted in 10 mM MOPS (pH 7) and adjusted to the desired salt concentrations with NaCl and $MgCl_2$: (A) TAR in 25 mM NaCl (triangles) and 334 mM NaCl (circles), (B) TAR in 0.1 mM $MgCl_2$ (triangles) and 0.5 mM $MgCl_2$ (circles), (C) AP-TAR in 25 mM NaCl (triangles) and 334 mM NaCl (circles), (D) AP-TAR in 0.1 mM $MgCl_2$ (triangles) and 0.5 mM $MgCl_2$ (circles), and (E) TAR in 0.1 mM $MgCl_2$ (triangles) and 0.1 mM $MgCl_2$ and 200 mM NaCl (circles).

likely to represent two independent transitions with very similar stabilities. Hence, the results suggest that, in the absence of $Mg^{2+}$, each of the helical regions in TAR unfolds independently. In contrast, in the presence of $Mg^{2+}$, all curves appear to unfold in a single transition, at both high and low $Mg^{2+}$ concentrations (Figure 4B). The results suggest cooperative unfolding of the


dx.doi.org/10.1021/bi200835t | *Biochemistry* 2011, 50, 9434–9445

**Table 1. Unfolding Enthalpies for Wild-Type TAR-RNA and AP-TAR RNA under Various Conditions[a]**

| conditions | $\Delta H_1$ (kcal) | $\Delta H_2$ (kcal) | $T_{M1}$ (°C) | $T_{M2}$ (°C) |
|---|---|---|---|---|
| | TAR RNA | | | |
| 25 mM NaCl | 36.5 | 36.5 | 60.5 | 62.3 |
| 71 mM NaCl | 45 | 51 | 58 | 70.5 |
| 200 mM NaCl | 38.4 | 44.5 | 60.5 | 75.5 |
| 334 mM NaCl | 45 | 52 | 62 | 77 |
| 560 mM NaCl | 50 | 58 | 66 | 79 |
| 0.05 mM $MgCl_2$, 25 mM NaCl | 42 | 42 | 64 | 65.8 |
| 0.1 mM $MgCl_2$, 25 mM NaCl | 42 | 42 | 67 | 68.5 |
| 0.5 mM $MgCl_2$, 25 mM NaCl | 49 | | 73 | |
| 1 mM $MgCl_2$, 25 mM NaCl | 53 | | 74.5 | |
| 0.1 mM $MgCl_2$, 71 mM NaCl | 42 | 49.5 | 60 | 71.3 |
| 0.1 mM $MgCl_2$, 200 mM NaCl | 47 | 53 | 63 | 76.3 |
| | AP-TAR | | | |
| 25 mM NaCl | 32 | 52.3 | 53 | 66 |
| 71 mM NaCl | 41 | 56 | 56 | 71.5 |
| 334 mM NaCl | 40 | 56 | 62 | 79.3 |
| 0.05 mM $MgCl_2$, 25 mM NaCl | 41 | 58 | 58 | 70.2 |
| 0.1 mM $MgCl_2$, 25 mM NaCl | 40 | 58 | 59 | 72 |
| 0.5 mM $MgCl_2$, 25 mM NaCl | 45 | 56 | 64.2 | 77.3 |

[a]All experiments were conducted in 10 mM MOPS (pH 7), which was adjusted to the desired salt concentration via addition of NaCl or $MgCl_2$.

stems in the presence of $Mg^{2+}$, likely due to stacking interactions in the three-nucleotide bulge and coaxial stacking of the two helices.[35,37,38] In the presence of 0.1 mM $Mg^{2+}$, the presence of high $Na^+$ concentrations (Figure 4C) promotes unfolding in two transitions, indicating that high $Na^+$ concentrations can compete with $Mg^{2+}$ for accumulation around the RNA, as expected for unspecific binding of ions. A summary of the $T_M$ values and unfolding enthalpies under each condition can be found in Table 1.

**Calorimetry.** On the basis of the nearest neighbors parameters for RNA,[39] the unfolding of TAR RNA is expected to yield 82 kcal/mol, resulting from seven canonical base stacking interactions. However, the model-dependent van't Hoff enthalpies listed in Table 1 range between 36 and 42 kcal. In the cases in which two independent transitions are observed, the sum of the two transitions yields the expected enthalpy of unfolding. However, at the lower salt concentrations, it is unclear whether the stems unfold with similar $T_M$ values or only one of the helical regions forms. Therefore, we have conducted model-independent calorimetry experiments (data not shown) to determine the actual enthalpy of unfolding associated with TAR RNA. Our calorimetry results reveal that the unfolding of TAR RNA in 10 mM MOPS (pH 7) yields an enthalpy of 67 kcal/mol, indicating that both of the stems of TAR form, even at very low ionic strengths. The results support the idea that single UV transitions correspond to the nearly simultaneous unfolding of the two helical regions.

**TAR RNA Folding versus AP-TAR RNA Folding.** The fluorescence experiments described below use AP-TAR (Figure 1B), a TAR hairpin in which U25 has been replaced with the fluorescent base 2-aminopurine (2-AP). Although AP-TAR unfolds with van't Hoff enthalpies similar to that of unmodified TAR (Table 1), its overall stability differs slightly from that of unmodified TAR. The main difference is that the transitions are less cooperative, exhibiting two transitions even in the presence of $Mg^{2+}$ (Figure 4C,D). The results suggest that the presence of 2-AP alters the stacking interactions around the three-nucleotide bulge and the resulting coaxial stacking of the helices. Because aminoglycosides bind at the helical region around and below the three-nucleotide bulge,[19] it is possible that the presence of 2-AP does not alter their binding. However, the results suggest that additional controls are needed to determine whether binding to AP-TAR accurately corresponds with binding to wild-type TAR.

**Antibiotic Binding and Salt Dependence.** The unfolding experiments summarized above suggest that TAR RNA is completely folded at 0.1 mM $Mg^{2+}$ or 140 mM $Na^+$. CD titrations at 140 mM $Na^+$ (Figure 5 and Table 2) indicate that

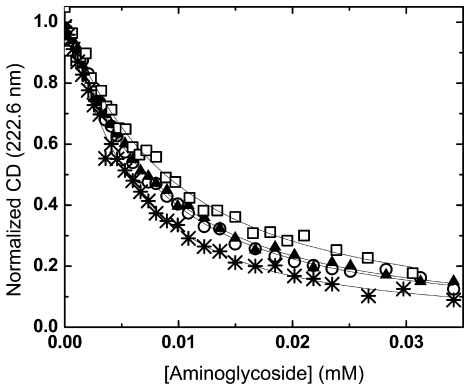


**Figure 5.** Circular dichroism titrations of TAR with kanamycin-B (○), paromomycin (▲), gentamycin (□), and tobramycin (∗). All experiments were conducted in 10 mM MOPS (pH 7) and 140 mM NaCl.

each of the four antibiotics binds with a slightly different affinity for TAR RNA. The binding affinities are marginally within the errors, but a trend can be observed in which tobramycin binds with the highest affinity and gentamycin binds with the lowest affinity (gentamycin < paromomycin < kanamycin-B < tobramycin). Because all these antibiotics have the same number of charges, the differences in binding affinities may reflect van der Waals interactions or H-bonds unique to each antibiotic. However, it is also possible that the difference in binding affinity reflects the extent of effective charge−charge interactions. It is possible that some antibiotics are able to orient their charges such that they make direct interactions with RNA groups while in other cases the geometry of the antibiotic prevents some charges from interacting directly with the RNA. The dependence of the binding affinity on salt concentration can be used to determine if the differences in affinity reflect differences in charge−charge interactions or other kinds of interactions. If the antibiotics exploit charge−charge interactions to the same extent, we would expect to see similar salt dependencies. However, if one antibiotic makes a more extensive array of charge−charge interactions, that antibiotic would be most affected by the increase in salt concentration, exhibiting a steeper slope in ln $K$ versus ln[$Na^+$] plots. Unfortunately, as the salt concentration increases, the change in CD signal at 222 nm upon addition of antibiotic decreases, and


dx.doi.org/10.1021/bi200835t | Biochemistry 2011, 50, 9434–9445

Table 2. Binding Affinities of Aminoglycosides for TAR-RNA Determined by Circular Dichroism[a]

| conditions | kanamycin-B ($\mu M^{-1}$) | paromomycin ($\mu M^{-1}$) | gentamycin ($\mu M^{-1}$) | tobramycin ($\mu M^{-1}$) |
|---|---|---|---|---|
| 140 mM NaCl | 0.220 ± 0.015 | 0.190 ± 0.012 | 0.160 ± 0.011 | 0.319 ± 0.085 |

[a]Experiments were conducted using total RNA concentrations of ~4 $\mu$M, in 10 mM MOPS buffer (pH 7) and 140 mM NaCl.

it becomes similar to the experimental error, especially in the presence $Mg^{2+}$. In addition, the changes in ellipticity upon antibiotic binding correspond to global conformational changes that occur upon antibiotic binding. Hence, the binding affinities obtained by CD reflect a coupled constant, which reports both the binding of antibiotics and the resulting conformational change ($K_{CD} = K_{bind}K_{conf}$). A coupled constant may be used to compare the differences in binding affinities only if all antibiotics undergo the same conformational change. Figure 6

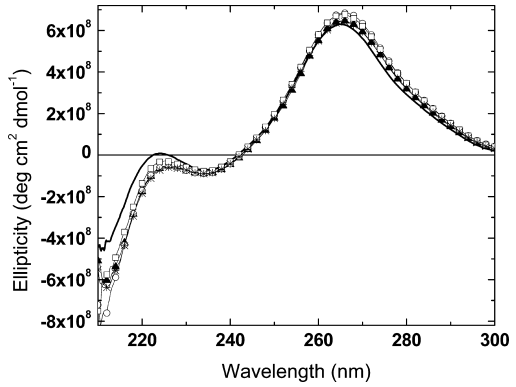


**Figure 6.** CD spectra of RNA (—) and RNA–antibiotic complexes [kanamycin-B (○), paromomycin (▲), gentamycin (□), and tobramycin (∗)]. The spectra of all complexes were recorded after saturation of the RNA with the corresponding antibiotic. All experiments were conducted in 10 mM MOPS (pH 7) and 140 mM NaCl.

shows the CD spectra of free TAR and TAR saturated with each of the antibiotics. Although the saturated spectra are very similar, there are some systematic deviations that may indicate slightly different conformational changes. Thus, to obtain the dependence of the binding affinity on $Na^+$, fluorescence binding experiments with kanamycin-B and paromomycin were conducted in 0.1 mM $Mg^{2+}$ and $Na^+$ concentrations in the range of 20–200 mM. The addition of 0.1 mM $Mg^{2+}$ to all samples is necessary to ensure that the RNA is folded. Panels A and B of Figure 7 show representative binding isotherms for the interactions between TAR and paromomycin and kanamycin-B, respectively. Figure 7C shows the dependence of $K$ on salt concentration. These results are summarized in Table 3. As expected, the binding affinities of kanamycin-B and paromomycin decrease as the concentration of $Na^+$ increases. However, the magnitude of this dependence differs between these two antibiotics, with kanamycin-B showing a stronger salt dependence than paromomycin.

**pH Titrations.** pH titrations (pH vs $[OH^-]$ profiles) were conducted for both paromomycin and kanamycin-B (data not shown). Each titration shows two pH jumps at pH ~4 and ~12. The first jump at pH 4 is not related to the aminoglycoside antibiotics; rather, it arises from our experimental procedure. Before the titrations were started, an excess of HCl was added to ensure that all the amino groups were protonated. Hence, the volume of KOH used to reach the first pH jump is simply the amount of KOH required to neutralize the excess HCl.

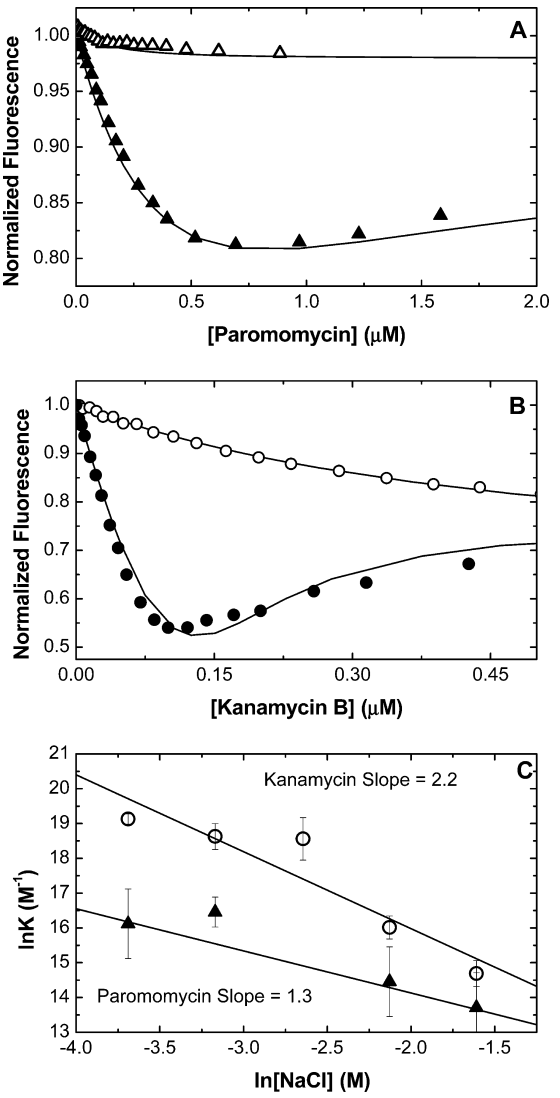


**Figure 7.** Binding of aminoglycosides to TAR-RNA. All experiments were conducted in 10 mM MOPS (pH 7) and 0.1 mM $MgCl_2$, and the desired salt concentrations were reached with NaCl. (A and B) Fluorescence binding isotherms at 200 mM NaCl (empty symbols) and 25 mM NaCl (filled symbols) for kanamycin-B (circles, panel B) and paromomycin (triangles, panel A). (C) Effect of NaCl on binding affinity for kanamycin-B (○) and paromycin (▲).

Once the excess HCl is removed, the pH jumps to a value of approximately 4, the value expected for a solution containing 99.9% protonated amino groups (calculated assuming a p$K_a$ of 7). This point marks the beginning of the titration. KOH added after this point removes protons from the amino groups of the antibiotics until all protons are removed and the second pH jump is reached. The concentration of antibiotics can be estimated from the volume of KOH required to go from the first to the second pH jump. The number of moles of KOH calculated from this volume is the same as the number of moles of amino groups present in solution, and the number of moles of antibiotic can be estimated by dividing the number of amino


dx.doi.org/10.1021/bi200835t | Biochemistry 2011, 50, 9434–9445

**Table 3. Binding Affinities for AP-TAR and Mixed RNAs Determined by Fluorescence**

| conditions | kanamycin-B ($\mu M^{-1}$) | paromomycin ($\mu M^{-1}$) |
|---|---|---|
| | AP-TAR RNA[a] | |
| 25 mM NaCl | 203 ± 30 | 10 ± 10 |
| 42 mM NaCl | 123 ± 46 | 14 ± 6 |
| 71 mM NaCl | 115 ± 70 | 15[b] |
| 119 mM NaCl | 9 ± 3 | 1.9 ± 1.4 |
| 200 mM NaCl | 2.4 ± 0.9 | 0.9 ± 1.3 |
| | AP-TAR and WT TAR RNA[a] | |
| 25 mM NaCl | 113 ± 38 | 10 ± 7 |
| 42 mM NaCl | 91 ± 30 | 22 ± 19 |
| 71 mM NaCl | 90 ± 31 | 13 ± 8 |
| 119 mM NaCl | 15 ± 4 | 2.3 ± 2.3 |
| 200 mM NaCl | 1.9 ± 0.1 | 2.8 ± 3.6 |

[a]Experiments were conducted using a total RNA concentration of ~0.2 $\mu$M, in 10 mM MOPS buffer (pH 7) containing 0.1 mM $MgCl_2$. The desired salt concentration was reached via addition of NaCl. [b]Because of technical problems, only one data set could be analyzed. This value was not included in the linear regression.

groups by 5 (the number of amino groups in the antibiotic). In addition to providing the concentration of each antibiotic (from the equivalence point), the results from these titrations provide an estimate of the p$K_a$ of each antibiotic (from the plateau regions, where the pH does not change significantly as the concentration of $OH^-$ ions increases). On the basis of these titrations, the p$K_a$ values of all the amino groups in kanamycin-B and paromomycin are similar, falling in the range of 7–9.

## DISCUSSION

**TAR RNA Folding.** Our UV melts show that TAR RNA unfolds in a single transition at low $Na^+$ concentrations but exhibits two transitions at $Na^+$ concentrations of >140 mM. These results combined with the calorimetry results suggest that although each of the stems of TAR forms at low $Na^+$ concentrations, they do not form optimally. At low $Na^+$ concentrations, the lower stem is likely to contain a partially unstacked base pair near the bulge. Hence, at low $Na^+$ concentrations, both stems have approximately three base stacks and exhibit similar stabilities (illustrated by their similar $T_M$ values). The reduction in the number of base pair stacks also explains the somewhat lower calorimetric enthalpy at low $Na^+$ concentrations (67 kcal vs the expected value of 82 kcal; the difference of ~15 kcal corresponds to one base pair stack). As the sodium concentration increases, two clear transitions are observed, suggesting that the bases of each stem are able to form better stacking interactions and fold completely, revealing their slightly different stabilities. Consistent with this picture, the binding affinity of neomycin as a function of $Na^+$ results in a hyperbolic plot, suggesting that in the absence of $Mg^{2+}$, TAR RNA does not fold completely at low $Na^+$ concentrations. When neomycin interacts with this imperfectly formed RNA, it binds with a relatively low affinity because its binding site may be compromised. As the concentration of $Na^+$ increases, the binding affinity of neomycin increases because its binding site is increasingly structured. Once a concentration of 140 mM $Na^+$ is reached, the stems are completely folded and cannot further fold. Additional increases in the $Na^+$ concentration interfere with the electrostatic interactions between TAR and neomycin, and from this point onward, the binding affinity decreases. Alternatively, the increase in affinity observed as the $Na^+$ concentration increases may be due to a decrease in the level of unspecific binding. From this point of view, the binding of neomycin at low salt concentrations would correspond to both specific neomycin–TAR interactions and nonspecific interactions between the positive charges in neomycin and the negatively charged RNA. As the salt concentration increases, the unspecific binding would be most affected and the neomycin molecules that were originally occupying the nonspecific site will be available for binding the specific site. This would increase the apparent binding affinity for the specific site simply because there is more neomycin that can bind this high-affinity site. As the concentration of $Na^+$ continues to increase, there would be less and less binding to the unspecific site until all molecules have been removed from this site. At this point, the apparent binding affinity would decrease because now we would be observing only the effect of $Na^+$ on a single, high-affinity, binding site. Although a decrease in the level of unspecific binding undoubtedly contributes to the observed increase in affinity, this contribution alone cannot explain the observed bell-shaped pattern. This is because the affinity increases ~6-fold from the lowest salt concentration to the peak of the bell-shaped plot in Figure 2. If this pattern was solely due to a decrease in the level of unspecific binding, this would mean that the unspecific site would have bound ~6 times more neomycin molecules than the specific site at low salt concentrations. Because the difference in binding affinity between the first and second neomycin binding sites is ~75-fold[27] and the TAR molecule used in our studies is not large enough to contain more than one or two unspecific sites, the unspecific site should not be able to sequester such a large amount of neomycin. Nevertheless, the bell-shaped plot observed in Figure 2 probably arises from both an increase in the fraction of TAR folded and a decrease in the level of unspecific binding.

UV melts in the presence of $Mg^{2+}$ show only one transition. The results suggest that stabilizing interactions at the three-nucleotide bulge promote coaxial stacking of the stems and stabilize the whole structure. When the temperature increases enough to destabilize these stabilizing interactions, the overall structure unfolds because at this temperature, both stems are past their corresponding $T_M$ values. Hence, the presence of $Mg^{2+}$ supports interactions that result in cooperative unfolding. Despite their different abilities to promote coaxial stacking of the TAR helices, our results suggest that both $Na^+$ and $Mg^{2+}$ bind unspecifically ("diffuse" ion binding[40]) because high concentrations of $Na^+$ seem to be able to outcompete $Mg^{2+}$ (as shown by the UV melts in the presence of 200 mM $Na^+$ and 0.1 mM $Mg^{2+}$). As seen for many other systems, $Na^+$ is simply less effective at stabilizing RNA tertiary contacts than $Mg^{2+}$.[40] The results imply that a very high concentration of $Na^+$ may be able to promote coaxial stacking of the TAR helices, consistent with previous reports.[36] Further support for this idea comes from closer inspection of the curves at very low $Mg^{2+}$ concentrations, where coaxial stacking seems to occur to a lesser degree than at higher $Mg^{2+}$ concentrations, further emphasizing the similarity between the effects of $Na^+$ and $Mg^{2+}$.

At low $Mg^{2+}$ concentrations, the derivative curves can be deconvoluted into two transitions with very similar $T_M$ values. Although the similarity of the $T_M$ values suggests cooperative unfolding of the stems, one may argue that concentrations below 0.1 mM $Mg^{2+}$ are not enough to promote stacking interactions in the three-nucleotide bulge and coaxial stacking of the two helices. This observation is consistent with the

results of our CD experiments. Hence, we can conclude that a minimum of 0.1 mM $MgCl_2$ is required to completely fold TAR, and therefore, all our titration experiments were conducted in 0.1 mM $MgCl_2$. It is important to note, however, that although the conformation of the three-nucleotide bulge and coaxial stacking of the helices may be slightly different in the presence of only $Na^+$ than in the presence of $Mg^{2+}$, the structure of TAR cannot be further folded beyond 140 mM $Na^+$, and at this high salt concentration, each helix is fully folded. Coaxial stacking is not required to obtain a fully structured TAR RNA capable of binding aminoglycoside antibiotics. Our main purpose is to fully fold the RNA helices so that we can measure the binding of antibiotics without further complications from concomitant helix folding. Thus, for example, the RNA in our CD titrations (conducted at 140 mM NaCl) contains two fully folded helices, although without cooperative coaxial stacking.

**TAR RNA Folding versus AP-TAR RNA Folding.** To follow the binding of antibiotic to TAR by fluorescence, we replaced U25 with 2-AP, as described by Marino.[27] Because the three-nucleotide bulge is likely to change upon binding of the antibiotic, the placement of 2-AP at this position ensures that the fluorescence signal will change upon antibiotic binding.[27] However, the presence of 2-AP at this position may also interfere with the tertiary contacts formed upon coaxial stacking of the TAR helices. Our UV melts suggest that although each of the stems forms like wild-type TAR, the conformation of the three-nucleotide bulge may have changed slightly. This is expected because U25 is part of the three-nucleotide bulge. To correct our fluorescence titrations for any deviation arising from the slightly different conformation, we conducted parallel titration experiments in which one cuvette contained only the labeled TAR (AP-TAR) while the second cuvette contained an equimolar mixture of AP-TAR and wild-type TAR. Our results show that AP-TAR slightly changes the binding affinity, but for most titrations, the change was within the experimental error. In general, aminoglycoside antibiotics bind AP-TAR with a slightly higher binding affinity. Aminoglycosides typically target RNA structures containing bulges,[21] and it has been suggested that their affinity for various RNA targets is related to the size of the asymmetric loops.[41] Hence, it is possible that the disruption of stacking interactions at the three-nucleotide bulge caused by the presence of the aminopurine base increases the flexibility of the bulge and makes it easier for aminoglycoside antibiotics to bind the lower stem of TAR, resulting in a slightly increased affinity. The results are consistent with the UV melts of AP-TAR, showing a decreased cooperativity under all conditions (illustrated by the presence of two transitions under all conditions), presumably resulting from changes in the stacking interactions around the three-nucleotide bulge. However, because aminoglycosides do not stack into the bulge but bind at the helical region below and around the bulge,[19] the difference in affinity is small and the trend observed for AP-TAR can be used to understand the behavior of wild-type TAR.

**Antibiotic Binding and Salt Dependence.** Our initial CD titrations show that although all the antibiotics that we used contained five charges, their affinities for TAR are different. The results suggest that the different position of the antibiotics charge results in different degrees of charge−charge interactions with TAR RNA. Although the binding affinities obtained by circular dichroism ($K_{CD}$) give us an idea of the relative affinity of each antibiotic for TAR RNA, CD may not the ideal technique for comparing the interactions between TAR and aminoglycosides because the values per se report on the global conformational change that is coupled to a binding event ($K_{CD} = K_{global\_conf}K_{bind}$). Hence, comparison of $K_{CD}$ values for the various antibiotics relies on having the same conformational change ($K_{global\_conf}$) for all TAR−antibiotic complexes. Although the CD spectra of all the antibiotic−TAR complexes (measured at the end of each titration, when the RNA is fully saturated) are similar (Figure 6), there are slight differences that may reflect a slightly different arrangement for each antibiotic. If that is the case, $K_{CD}$ values may not be useful for strictly comparing the binding affinities. Consistent with this idea, it is worth noting that the values obtained by circular dichroism are ~1000-fold lower than the values obtained by fluorescence, probably reflecting the fact that circular dichroism reports on a global conformational change (with low $K_{global\_conf}$, reflecting a substantial and difficult change), while our fluorescence experiments report on the local stacking of the aminopurine base, which is a small change and is likely to be similar for all antibiotics because it results directly from the binding of aminoglycosides and hence more accurately reports on the binding event ($K_{fluorescence} = K_{local\_conf}K_{bind}$, where $K_{local\_conf}$ reflects a local, more permissible change, perhaps leaving $K_{fluorescence}$ similar to $K_{bind}$). In addition, the ellipticity at 222 nm changes significantly upon TAR RNA folding (for instance, it decreases as we add $Na^+$ or $Mg^{2+}$). The signal continues to decrease upon addition of the antibiotics, but at high salt concentrations, the change in signal is small and the experimental error becomes significant, increasing the uncertainty of our measurements. Finally, on the basis of the fluorescence results, it is clear that there is a secondary, unspecific binding site. Thus, depending on the specific salt concentration, the binding affinities obtained by CD may also include the binding to this unspecific site. Hence, although CD was useful for providing an initial indication that there were differences in the interaction between these antibiotics and TAR, it is not the ideal technique for comparing the binding affinities of different antibiotics.

**Antibiotic p$K_a$.** One possible explanation for the difference in salt dependence between kanamycin-B and paromomycin may be related to the p$K_a$ values of their amino groups. If the p$K_a$ values of kanamycin-B are higher than the p$K_a$ values of paramomycin, the amino groups of kanamycin-B will be protonated to a larger extent at pH 7. With a higher percentage of protonated amino groups, the overall charge of kanamycin-B will be larger, explaining the difference in affinity solely on the basis of unspecific electrostatic interactions. The results of our pH titrations indicate that the p$K_a$ values of all the amino groups in both paromomycin and kanamycin-B are in the range of 7−9. Hence, because the titration profiles are very similar, it is reasonable to assume that the overall charges of these antibiotics are similar at pH 7. Furthermore, although the difference between titrations is within the error, the p$K_a$ values of paromomycin are slightly higher than the p$K_a$ values of kanamycin-B, confirming that the increase in affinity of kanamycin-B cannot be explained by a larger degree of protonation.

**Comparison with Previous Reports.** Our fluorescence experiments in the presence of 0.1 mM $Mg^{2+}$ and various $Na^+$ concentrations further support the idea that the difference in binding affinities reflects differences in charge−charge interactions. Kanamycin-B has a stronger salt dependence than paromomycin, which binds TAR with a lower affinity. The

results suggest that the differences in the positions of the charges result in optimal charge−charge interactions in the case of kanamycin-B, while these interactions are suboptimal in the case of paromomycin. Unfortunately, there are no published structures for the TAR−kanamycin or TAR−paromomycin complexes with which we can determine whether the charges of kanamycin make more optimal interactions with TAR RNA. However, the possibility of more optimal interactions between kanamycin and TAR is consistent with previous observations of the binding of kanamycin and paromomycin to the ribosomal A-site (Protein Data Bank entries IJ7T[42] and 2ESI[43]), which show that kanamycin can position four of its charges very close (within 3.5 Å) to the RNA groups while paramomycin can position only three of its charges near the RNA. Although these experiments were conducted using a different RNA, the results suggest that one of the possible kanamycin conformations is able to position its groups near the RNA. The experiments described in ref 43 use kanamycin-A, which is identical to kanamycin-B except that one amino group is replaced by an alcohol and therefore has only four charges. Although this may indicate that the fifth charge of kanamycin-B may further contribute to the electrostatic interactions between kanamycin and TAR, on the basis of the structure in ref 43, this group would end up being too far from the RNA. Nevertheless, with four charges making close charge−charge interactions with RNA groups, kanamycin is able to exploit electrostatic interactions to a great extent.

Two additional studies support the idea that differences in the extent of optimal charge−charge interactions could lead to significant differences in binding affinities. First, a study of the interactions between aminoglycosides and TAR[44] shows that kanamycin-A and kanamycin-B bind TAR RNA with similar binding affinities, despite the fact that kanamycin-B has one additional charge (the $K_d$ values are 89 ± 10 $\mu$M for kanamycin-B and 107 ± 13 $\mu$M for kanamycin-A under the conditions described in ref 44). This result is consistent with our suggestion that the fifth charge in kanamycin-B would end up being too far from the RNA to make a direct charge−charge interaction and suggests that kanamycin may bind TAR and the A-site with a similar geometry. The second study shows the NMR structure of neomycin bound to TAR RNA (Protein Data Bank entry 1QD3).[19] Because paromomycin is very similar to neomycin [they differ in only one amino group; hence, neomycin has one more charge than paromomcyin (see Figure 1)], one would expect paromomycin and neomycin to bind TAR in a similar way. On the basis of the structure of the neomycin−TAR complex, paromomycin would be able to place only three of its five amino charges near the RNA groups (within 3.5 Å), suggesting again that the geometry of paromomycin does not allow this antibiotic to make as many optimal contacts as kanamycin. This is also consistent with the 12-fold decrease in affinity going from neomycin (which can place four of its charged groups near the RNA) to paromomycin.[44] It is interesting to see that the three charges paromomycin can place near TAR RNA are not the same charges paromomycin places near the A-site. Paromomycin binds the A-site using the amino groups in rings II−IV, while it uses rings I−III to bind TAR RNA. The actual orientation of paromomycin in TAR RNA will need to await the publication of an NMR or crystal structure, but it is interesting to see that in both orientations only three charges closely approach the RNA.

**Implications for Drug Design: Charges Are Not the Whole Story.** Our results suggest that the position of the charges makes a significant contribution to the binding affinity. Furthermore, this concept may explain why a simple examination of the number of charges does not explain the trends in $IC_{50}$ values observed for aminoglycoside antibiotics.[18] For example, streptomycin (three charges) was found to be more effective than gentamycin (five charges) at inhibiting the interactions between TAR and Tat.[18] We speculate that perhaps the charges in streptomycin are more optimally positioned than those in gentamycin.

Although our results suggest that the design of inhibitors of the TAR−Tat interactions should consider not only the number of charges but also their specific position in the molecules, it is worth emphasizing that other interactions are also important in the binding of aminoglycoside. For example, tobramycin binds with higher affinity than kanamycin-B (Table 2 and ref 44), even though their charges are in the same positions. The only difference between kanamycin-B and tobramyin is the presence of an extra OH group in tobramycin, suggesting that the formation of an additional hydrogen bond could result in further optimization of tobramycin−TAR contacts. Finally, the presence of an additional hydrogen bond can also contribute to the large difference in binding affinity between neomycin and ribostamycin (~60-fold difference according to ref 44). The only difference between neomycin and ribostamycin is that ribostamycin does not contain ring IV, but the charges in this ring are too distant to make direct contacts with TAR (based on Protein Data Bank entry 1QD3[19]). However, one of the OH groups in ring IV is close enough to make a hydrogen bond with G43, suggesting that the additional hydrogen bond could contribute to optimizing the interactions between neomycin and TAR.

**Technical Remarks.** The binding affinities reported here depend heavily on two factors: the exact antibiotic concentrations and the accuracy of our fitting procedures. Thus, it is worth summarizing the steps we took in obtaining accurate values for these procedures.

Each antibiotic was purchased from Sigma, and the certificate of analysis was initially used to calculate a molecular weight. This is necessary because the antibiotics contain variable amounts of sulfate ions as counterions, but the exact amount depends on the degree of protonation of the amino groups at the time of crystallization. The percentage of carbon, nitrogen, and sulfur (from Sigma's certificate of analysis) can be used to estimate the molecular weight. However, small variations in these percentages (within the reported acceptable ranges) can significantly change the molecular weight, and the molecular weights determined from C, N, and S vary approximately 20% from each other. Thus, we conducted pH titrations to determine the exact molecular weight of each batch. The molecular weights determined in our pH titrations were in the same range as the values calculated on the basis of the percentages of C, S, and N, suggesting that our analysis provides a reasonable estimate of the molecular weights.

The values of the binding affinities also depend on the model used for such analysis. Here we assumed that we have two independent binding sites, one with a higher affinity than the other. A brief description of the model used can be found in Experimental Procedures, but we would like to make some remarks about the fitting procedures and our interpretation of $K_1$ and $K_2$. Because the curves at low $Na^+$ concentrations show a gradual decrease in fluorescence followed by a gradual

increase, we have assumed the presence of a second binding site at low $Na^+$ concentrations, which has been reported previously.[27] We believe that this secondary binding site is unspecific because it disappears at high $Na^+$ concentrations, suggesting that $Na^+$ can compete with the antibiotics for this secondary binding site. Hence, this site may reflect unspecific charge−charge interactions between the RNA and the charged aminoglycosides. To fit the titration curves collected al low $Na^+$ concentrations accurately, a program capable of handling a very large equation is needed. Our analysis used the program ProFit (QuantumSoft). This program was able to fit our data according to the equation described in Experimental Procedures, yielding values for the binding affinities ($K_1$ and $K_2$) and the proportionality coefficients (equivalent to UV extinction coefficients) of TAR in its different bound states (free, bound to one ligand, and bound to two ligands). Because there are so many variables in this fitting procedure, the errors for the binding affinities are somewhat large; hence, care has been taken to report the average of at least two experiments and as many as four, when necessary. Despite the large errors, it is clear that kanamycin-B binds TAR with higher affinity than paromomycin.

## CONCLUSIONS

Because many of the biological functions of RNA depend on its conformation,[45] it is important to understand how specific conformations may affect the interactions of RNA with various ligands. Because RNA is highly negatively charged, each conformation places the phosphate and other electronegative groups at specific positions in space. Although electrostatic interactions are sometimes regarded as nonspecific, the RNA electrostatic surface may be exploited in the design of drugs that target RNA, as has been suggested previously.[46] Numerous studies have shown that TAR RNA can adopt a coaxially stacked conformation in the presence of various ligands ranging from divalent ions[35,36,38] to small cationic ligands.[19,37,46] Electrostatic calculations using the nonlinear Poisson−Boltzmann equation[36,46] have shown that these coaxially stacked conformations contain regions of strong negative electrostatic potential, which require stabilization by cationic ligands. Furthermore, previous studies have shown that a synthetic ligand (rbt203 in ref 46) can bind TAR with high affinity by positioning its cationic groups near the electrostatic regions of negative potential. However, another ligand (rbt158 in ref 46) binds with much lower affinity, presumably because it cannot place its cationic groups as optimally as rbt203. These results suggest that ligands that are flexible enough to position their cationic groups exactly at the electrostatic "hot spots" are better able to stabilize the bound conformation and bind TAR with higher affinity. Our results provide additional evidence to support this concept. The position of the charges in aminoglycoside antibiotics and the flexibility of their structure, rather than the number of charges, determine whether an antibiotic will be able to bind with high affinity to TAR RNA. Our overall results show that the two antibiotics tested display a different dependence of the binding affinity on salt concentration. Because both antibiotics have five charges, the results suggest that the charges of these antibiotics are oriented in a different way when bound to TAR RNA. Hence, the specific position of the charges should be considered in the design of any inhibitor of the TAR−Tat interaction.

## AUTHOR INFORMATION


### Corresponding Author

*E-mail: asoto@towson.edu. Phone: (410) 704-2605. Fax: (410) 704-4265.

### Present Address

[§]Loreal USA Inc., 159 Terminal Ave., Clark, NJ 07066.



### Funding

This work was supported by a Henry C. Welcome Fellowship (A.M.S.), Towson University Start Up Funds (A.M.S.), a Towson University Faculty Development and Research Committee Grant (A.M.S.), Ronald and Linda Raspet Fellowships (A.L.S. and K.J.S.), and The College of New Jersey Summer Research Fellowship (J.K.) and Start Up funds (A.M.S.).


## ACKNOWLEDGMENTS


We thank Dr. David Draper for his constant advice and for allowing us to use several instruments in his laboratory, Dr. Stephen Scales for editorial revisions of the manuscript, Mr. George Kram and Ms. Leetta Abner for their assistance with the various supplies needed throughout this work, and the two anonymous reviewers of this manuscript for their helpful comments and suggestions.


## ABBREVIATIONS

CD, circular dichroism; TAR RNA, transactivator responsive region (TAR) RNA; AP-TAR, aminopurine-TAR; 2-AP, 2-aminopurine; $T_M$, "melting" temperature (unfolding temperature); $K_{CD}$, binding affinity measured by circular dichroism; $K_{global\_conf}$, equilibrium constant corresponding to a global conformational change; $K_{bind}$, binding affinity; $K_{local\_conf}$, equilibrium contant corresponding to a local conformational change; $K_{fluorescence}$, binding affinity measured by fluorescence.

## REFERENCES


(1) Cooper, T. A., Wan, L., and Dreyfuss, G. (2009) RNA and disease. *Cell 136*, 777−793.

(2) Gottfredsson, M., and Bohjanen, P. R. (1997) Human immunodeficiency virus type I as a target for gene therapy. *Front. Biosci. 2*, 619−634.

(3) Gallego, J., and Varani, G. (2001) Targeting RNA with small-molecule drugs: Therapeutic promise and chemical challenges. *Acc. Chem. Res. 34*, 836−843.

(4) Muesing, M. A., Smith, D. H., and Capon, D. J. (1987) Regulation of mRNA accumulation by a human immunodeficiency virus trans-activator protein. *Cell 48*, 691−701.

(5) Sharp, P. A., and Marciniak, R. A. (1989) HIV TAR: An RNA enhancer? *Cell 59*, 229−230.

(6) Feng, S., and Holland, E. C. (1988) HIV-1 tat trans-activation requires the loop sequence within tar. *Nature 334*, 165−167.

(7) Fanales-Belasio, E., Raimondo, M., Suligoi, B., and Buttò, S. (2010) HIV virology and pathogenetic mechanisms of infection: A brief overview. *Ann. Ist. Super. Sanita 46*, 5−14.

(8) Fulcher, A. J., and Jans, D. A. (2003) The HIV-1 Tat transactivator protein: A therapeutic target? *IUBMB Life 55*, 669−680.

(9) Cullen, B. R. (1986) Trans-activation of human immunodeficiency virus occurs via a bimodal mechanism. *Cell 46*, 973−982.

(10) Karn, J. (2000) Tat, a novel regulator of HIV transcription and latency. HIV sequence database from Los Alamos National Laboratory (http://www.hiv.lanl.gov/content/sequence/HIV/REVIEWS/KARN2000/Karn.html).

(11) Karn, J. (1999) Tackling Tat. *J. Mol. Biol. 293*, 235−254.

(12) Dingwall, C., Ernberg, I., Gait, M. J., Green, S. M., Heaphy, S., Karn, J., Lowe, A. D., Singh, M., Skinner, M. A., and Valerio, R. (1989)

Human immunodeficiency virus 1 tat protein binds trans-activation-responsive region (TAR) RNA in vitro. *Proc. Natl. Acad. Sci. U.S.A. 86*, 6925−6929.
(13) Tahirov, T. H., Babayeva, N. D., Varzavand, K., Cooper, J. J., Sedore, S. C., and Price, D. H. (2010) Crystal structure of HIV-1 Tat complexed with human P-TEFb. *Nature 465*, 747−751.
(14) Isel, C., and Karn, J. (1999) Direct evidence that HIV-1 Tat stimulates RNA polymerase II carboxyl-terminal domain hyperphosphorylation during transcriptional elongation. *J. Mol. Biol. 290*, 929−941.
(15) Kao, S. Y., Calman, A. F., Luciw, P. A., and Peterlin, B. M. (1987) Anti-termination of transcription within the long terminal repeat of HIV-1 by tat gene product. *Nature 330*, 489−493.
(16) Hermann, T., and Westhof, E. (1999) Docking of cationic antibiotics to negatively charged pockets in RNA folds. *J. Med. Chem. 42*, 1250−1261.
(17) Bloomfield, V. A., Crothers, D. M., and Tinoco, I. (2000) *Protein-Nucleic Acids Interactions*, University Science Books, Sausalito, CA.
(18) Mei, H. Y., Galan, A. A., Halim, N. S., Mack, D. P., Moreland, D. W., Sanders, H. N., Truong, H. N., and Czarnik, A. W. (1995) Inhibition of an HIV-Tat derived peptide binding to TAR RNA by aminoglycoside antibiotics. *Bioorg. Med. Chem. Lett. 5*, 2755−2760.
(19) Faber, C., Sticht, H., Schweimer, K., and Rösch, P. (2000) Structural rearrangements of HIV-1 Tat-responsive RNA upon binding of neomycin B. *J. Biol. Chem. 275*, 20660−20666.
(20) Wang, S., Huber, P. W., Cui, M., Czarnik, A. W., and Mei, H. Y. (1998) Binding of neomycin to the TAR element of HIV-1 RNA induces dissociation of Tat protein by an allosteric mechanism. *Biochemistry 37*, 5549−5557.
(21) Chittapragada, M., Roberts, S., and Ham, Y. W. (2009) Aminoglycosides: Molecular insights on the recognition of RNA and aminoglycoside mimics. *Perspect. Med. Chem. 3*, 21−37.
(22) García-García, C., and Draper, D. E. (2003) Electrostatic interactions in a peptide-RNA complex. *J. Mol. Biol. 331*, 75−88.
(23) Chin, K., Sharp, K. A., Honig, B., and Pyle, A. M. (1999) Calculating the electrostatic properties of RNA provides new insights into molecular interactions and function. *Nat. Struct. Biol. 6*, 1055−1061.
(24) Marky, L. A., and Breslauer, K. J. (1987) Calculating thermodynamic data for transitions of any molecularity from equilibrium melting curves. *Biopolymers 26*, 1601−1620.
(25) Draper, D. E., and Gluick, T. C. (1995) Melting studies of RNA unfolding and RNA-ligand interactions. *Methods Enzymol. 259*, 281−305.
(26) Draper, D. E., Bukhman, Y. V., and Gluick, T. C. (2001) Thermal methods for the analysis of RNA folding pathways. *Current Protocols in Nucleic Acid Chemistry*, Chapter 11, Unit 11.3, Wiley, New York.
(27) Bradrick, T. D., and Marino, J. P. (2004) Ligand-induced changes in 2-aminopurine fluorescence as a probe for small molecule binding to HIV-1 TAR RNA. *RNA 10*, 1459−1468.
(28) Bausch, S. L., Poliakova, E., and Draper, D. E. (2005) Interactions of the N-terminal domain of ribosomal protein L11 with thiostrepton and rRNA. *J. Biol. Chem. 280*, 29956−29963.
(29) Wiseman, T., Williston, S., Brandts, J. F., and Lin, L. N. (1989) Rapid measurement of binding constants and heats of binding using a new titration calorimeter. *Anal. Biochem. 179*, 131−137.
(30) ITC Data Analysis in Origin, Tutorial Guide, version 5 (1998) Microcal.
(31) Wang, Z. X., and Jiang, R. F. (1996) A novel two-site binding equation presented in terms of the total ligand concentration. *FEBS Lett. 392*, 245−249.
(32) Nelson, D. L., and Cox, M. M. (2004) *Lehninger Principles of Biochemistry*, 4th ed., pp 278, W. H. Freeman, New York.
(33) Fox, J. J., Wempen, I., Hampton, A., and Doerr, I. L. (1958) Thiation of Nucleosides. I. Synthesis of 2-Amino-6-mercapto-9-β-D-ribofuranosylpurine ("Thioguanosine") and Related Purine Nucleosides. *J. Am. Chem. Soc. 80*, 1669−1675.
(34) Weeks, K. M., Ampe, C., Schultz, S. C., Steitz, T. A., and Crothers, D. M. (1990) Fragments of the HIV-1 Tat protein specifically bind TAR RNA. *Science 249*, 1281−1285.
(35) Ippolito, J. A., and Steitz, T. A. (1998) A 1.3 Å resolution crystal structure of the HIV-1 transactivator response region RNA stem reveals a metal ion dependent bulge conformation. *Proc. Natl. Acad. Sci. U.S.A. 95*, 9819−9824.
(36) Casiano-Negroni, A., Sun, X., and Al-Hashimi, H. M. (2007) Probing $Na^+$-induced changes in the HIV-1 TAR conformational dynamics using NMR residual dipolar couplings: New insights into the role of counterions and electrostatic interactions in adaptive recognition. *Biochemistry 46*, 6525−6535.
(37) Pitt, S. W., Majumdar, A., Serganov, A., Patel, D. J., and Al-Hashimi, H. M. (2004) Argininamide binding arrests global motions in HIV-1 TAR RNA: Comparison with $Mg^{2+}$-induced conformational stabilization. *J. Mol. Biol. 338*, 7−16.
(38) Al-Hashimi, H. M., Pitt, S. W., Majumdar, A., Xu, W., and Patel, D. J. (2003) $Mg^{2+}$-induced variations in the conformation and dynamics of HIV-1 TAR RNA probed using NMR residual dipolar couplings. *J. Mol. Biol. 329*, 867−873.
(39) Xia, T., SantaLucia, J. Jr., Burkard, M. E., Kierzek, R., Schroeder, S. J., Jiao, X., Cox, C., and Turner, D. H. (1998) Thermodynamic parameters for an expanded nearest-neighbor model for formation of RNA duplexes with Watson-Crick base pairs. *Biochemistry 37*, 14719−14735.
(40) Draper, D. E. (2004) A guide to ions and RNA structure. *RNA 10*, 335−343.
(41) Ryu, D. H., and Rando, R. R. (2002) Decoding region bubble size and aminoglycoside antibiotic binding. *Bioorg. Med. Chem. Lett. 12*, 2241−2244.
(42) Vicens, Q., and Westhof, E. (2001) Crystal structure of paromomycin docked into the eubacterial ribosomal decoding A site. *Structure 9*, 647−658.
(43) François, B., Russell, R. J., Murray, J. B., Aboul-ela, F., Masquida, B., Vicens, Q., and Westhof, E. (2005) Crystal structures of complexes between aminoglycosides and decoding A site oligonucleotides: role of the number of rings and positive charges in the specific binding leading to miscoding. *Nucleic Acids Res. 33*, 5677−5690.
(44) Blount, K. F., and Tor, Y. (2003) Using pyrene-labeled HIV-1 TAR to measure RNA-small molecule binding. *Nucleic Acids Res. 31*, 5490−5500.
(45) Batey, R. T., Rambo, R. P., and Doudna, J. A. (1999) Tertiary Motifs in RNA Structure and Folding. *Angew. Chem., Int. Ed. 38*, 2326−2343.
(46) Davis, B., Afshar, M., Varani, G., Murchie, A. I., Karn, J., Lentzen, G., Drysdale, M., Bower, J., Potter, A. J., Starkey, I. D., Swarbrick, T., and Aboul-ela, F. (2004) Rational design of inhibitors of HIV-1 TAR RNA through the stabilisation of electrostatic "hot spots". *J. Mol. Biol. 336*, 343−356.